Illumination Estimation Based on Valid Pixel Selection from CCD Camera Response

Oh-Seol Kwon,▲ Yang-Ho Cho,▲ and Yeong-Ho Ha▲†
School of Electrical Engineering and Computer Science, Kyungpook National University, Daegu, KOREA

Yun-Tae Kim
Digital Research Center, Samsung Advanced Instituite of Technology, Yongin, KOREA

This article proposes a method for estimating the illuminant chromaticity using the distributions of the camera responses obtained by a CCD camera in a real world scene. Illumination estimation using a highlight method is based on the geometric relation between a body and its surface reflection. In general, the pixels in a highlight region are affected by an illuminant geometric difference, camera quantization errors, and the non-uniformity of the CCD sensor. As such, this leads to inaccurate results if an illuminant chromaticity is estimated using the pixels of a CCD camera without any preprocessing. Accordingly, to solve this problem, the proposed method analyzes the distribution of the CCD camera responses and selects pixels by the Mahalanobis distance in highlight regions. The use of the Mahalanobis distance based on the camera responses enables the adaptive selection of valid pixels among the pixels distributed in the highlight regions. A principal component analysis (PCA) is then used to determine the lines based on the $r - g$ chromaticity coordinates of the selected pixels. Thereafter the illuminant chromaticity is estimated based on the intersection points of the lines. Experimental results using the proposed method demonstrated a reduced estimation error compared with conventional methods.

Journal of Imaging Science and Technology 49: 308–316 (2005)

Introduction

The color of an object from reflected light is determined by the spectral power distribution of the illumination and surface reflectance of the object and the grade of the receptor's response. As such, if illumination characteristics could be estimated, such as the spectral power distribution or chromaticity values of an illumination, this information could be effectively applied to a variety of areas, such as pattern recognition, image processing, color appearance modeling, and so on. In the case of human beings, the original color of an object under an arbitrary illumination is estimated as an integrated judgment. Consequently, in practice the scene is corrected by the human visual system. However an input device, such as a camera, is unable to discriminate the features of the original input responses, leaving a need for illumination estimation to replicate the visual ability of humans.

Illumination estimation methods can be classified according to whether they use spectral reflectance[1–7] or a tristimulus.[8–11] The basic approach using spectral reflectance was originally designed by Maloney,[1] where the spectral reflection from an object surface comes from multiplying the body and the surface reflection, allowing the spectral reflectance of an illumination to be estimated using an analysis of this multiplication formula. Thereafter D'Zmura[2] proposed general linear and bilinear models to extend Maloney's approach based on the combination of multiple illuminations and multiple surfaces and the relationship between these two factors. Plus, Tominaga[3] proposed the method of illumination estimation using singular value decomposition, while Forsyth[4] introduced the concept of a canonical gamut to solve the color problem, where a canonical gamut consists of all possible combinations of the real illumination and surface reflectance, which allows the illumination and surface reflectance to be estimated by analyzing the relationship between arbitrary reflectance and the canonical gamut. More recently, illumination classification methods have been proposed to reduce the complexity of the computation when illumination information can be obtained. For example, Wandell[5] and Tominaga[6] estimate the power spectral distribution using the concept of a blackbody, yet here the illumination is classified according to the gamut for the scene, which results in a regular error. Thus, accurate illumination estimation is needed.

In contrast, Land's Retinex theory[8] uses a tristimulus input along with the gray world assumption that the average vector for the three channels is assumed to be the

Original manuscript received March 31, 2004

▲ IS&T Member

†Corresponding Author: Y.-H. Ha, yha@ee.knu.ac.kr

Supplemental Material—Figures 2, 3 and 6 through 9 can be found in color on the IS&T website (www.imaging.org) for a period of no less than two years from the date of publication.

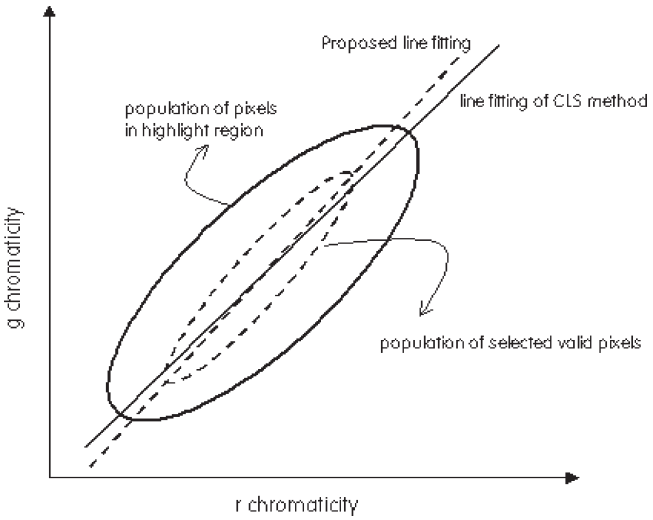

Figure 1. Example of line detection in highlight region.

illuminant chromaticity for the scene or image. Other approaches using highlights have also been considered. For example, Shafer[9] proposed the dichromatic reflection model, which includes two vector components: surface reflection and body reflection. The vector addition of these weighted components then allows the light reflection to be represented using the object surface, based on the assumption that the spectral composition of the surface reflection is the same as the illuminant spectrum. Plus, since the chromaticity distribution of pixels in a highlight region makes line patterns from the surface to the illuminant chromaticity or vice versa, a point on the line can be represented as the linear combination of the body and the illuminant chromaticity vector. Lee[10] also proposed a method for estimating the illuminant chromaticity by analyzing regions with a chromaticity change, i.e., for highlight regions in an image, the chromaticity distribution of the highlight region makes a line (IPS method), and if there are more than two lines, the cross point is assumed to be the illuminant chromaticity. Recently, Tan proposed a method of illumination estimation using the inverse-intensity chromaticity space (Inverse-Intensity method).[11] Tan's method creates a two-dimensional space that can be applied without segmenting the colors in the image. This algorithm can also be applied to highly textured surfaces.

Since Lee's method basically estimates an illumination with either a synthetic or optimal image, it is difficult to obtain a good result for a real world scene, as the camera responses include quantization errors and nonuniform CCD sensors.[12] Therefore to overcome this problem, Lehmann[13] recently proposed an illumination estimation method for real world scenes that uses an additional 20 images to compensate for the camera noise. Lehmann's method, Color Line Search (CLS), consists of three steps. First, the highlight regions are automatically selected and their pixels transformed into chromaticity coordinates. Second, the color lines are determined according to the dichromatic reflectance using a Hough transform. Third, a consistency check is applied based on a corresponding path search of the image domain. Yet, this method cannot be applied when additional images are unobtainable.

Accordingly, this article proposes an illumination estimation method using the Mahalanobis distance that considers the camera response distribution in a single image. In general, the pixels in a highlight region consist of a group of $r-g$ chromaticity coordinates with an elliptical shape, which is why they are influenced by various factors, including camera noise. Figure 1 shows an example of line detection when using all the pixels in a highlight region and only selected valid pixels, emphasizing the difference in the resulting line detection.

Therefore, this article surveys the camera response distribution for the total color regions and proposes a method for valid pixel selection in highlight regions after calculating the Mahalanobis distance for the distribution characteristic. Thereafter, a Principal Component Analysis (PCA) is used to make a line for the selected pixels in a highlight region and the illumination estimated based on the line points.

Illumination Estimation Using Highlight Region

Illumination estimation using a highlight region is based on using the illumination information captured by the chromaticity distribution of the pixels in a highlight region. This method is relatively straightforward and frequently used, as an illumination can be estimated based on the output response without any specific camera optics. The camera input response[14] is indicated by the following equation:

$$C_k = \int_{\varpi} e(\lambda)s(\lambda)\psi(\lambda)d\lambda, \tag{1}$$

where C_k is the RGB value of the camera response, $e(\lambda)$ is the spectral power distribution, $s(\lambda)$ is the sensitivity of the camera, and $\psi(\lambda)$ is the surface reflectance. Equation (1) can also be divided by the interface reflectance and body reflectance, and described by a dichromatic reflection model[8] as follows:

$$C_k = \alpha(\theta)C_S + \beta(\theta)C_B, \tag{2}$$

where θ is determined based on the difference between the illumination orientation and the normal vector of the surface, α,β are geometrical factors, and C_S and C_B are the interface reflectance and body reflectance of the object, respectively. Thus, Eq. (1) can be represented as follows:

$$C_k = \alpha(\theta)\int_{\varpi} e(\lambda)s(\lambda)\psi(\lambda)d\lambda + \beta(\theta)\int_{\varpi} e(\lambda)s(\lambda)\psi(\lambda)d\lambda, \tag{3}$$

Equation (3) is described using RGB values,

$$\begin{pmatrix} R \\ G \\ B \end{pmatrix} = \alpha(\theta)\begin{pmatrix} R \\ G \\ B \end{pmatrix}_I + \beta(\theta)\begin{pmatrix} R \\ G \\ B \end{pmatrix}_B, \tag{4}$$

where the interface reflectance part I is considered the same as the illumination irradiating the object in the scene; r and g are defined by normalizing the sum of R, G, and B for the camera-specific RGB color space.

$$\begin{pmatrix} r \\ g \end{pmatrix} = \begin{pmatrix} \dfrac{R}{R+G+B} \\ \dfrac{G}{R+G+B} \end{pmatrix}. \tag{5}$$

Equation (5) is substituted for $(R,G,B)^T$ computed by Eq. (4).

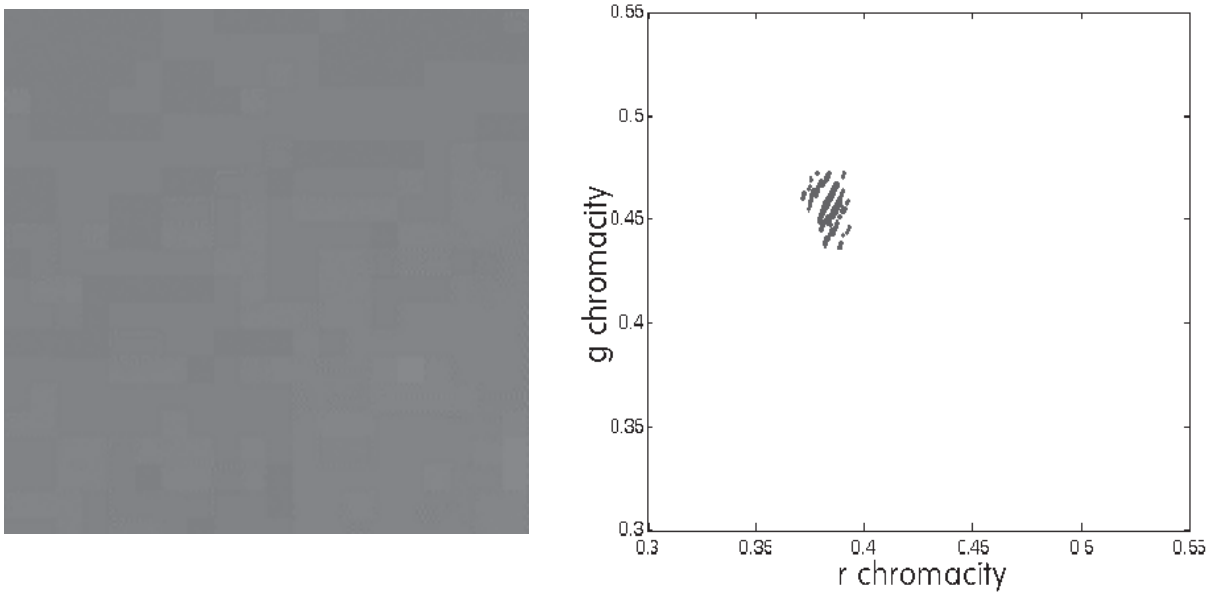

(a) (b)

Figure 2. CCD camera response for uniform patch; (a) uniform green patch and (b) camera response distribution based on $r-g$ chromaticity coordinates. *Supplemental Material—Figure 2 can be found in color on the IS&T website (www.imaging.org) for a period of no less than two years from the date of publication.*

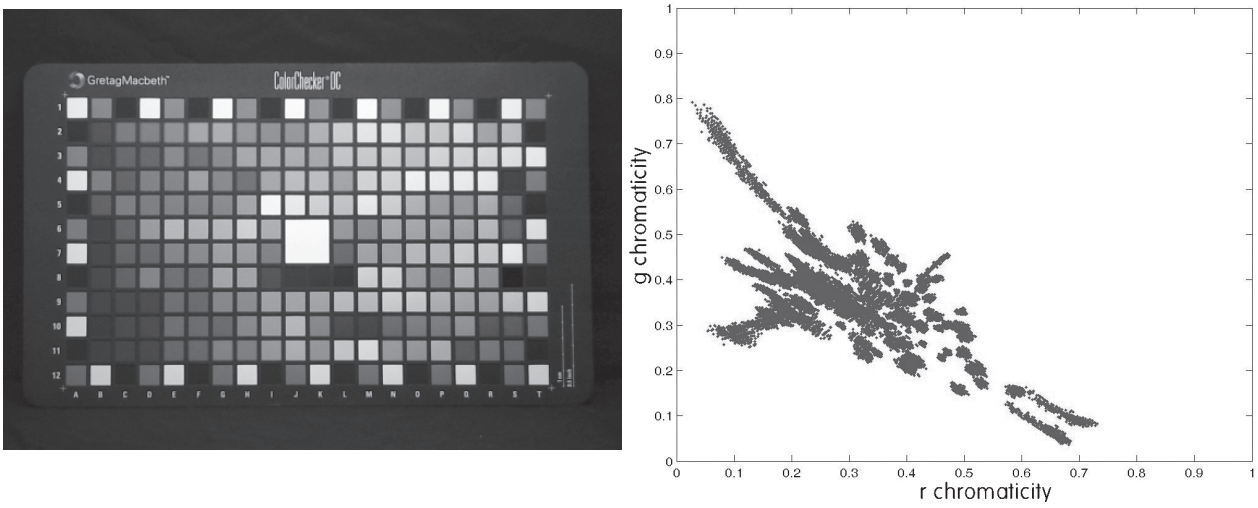

(a) (b)

Figure 3. Distribution of CCD camera response based on $r-g$ chromaticity coordinates; (a) Gretag Macbeth Color Checker and (b) response distribution based on $r-g$ chromaticity coordinates. *Supplemental Material—Figure 3 can be found in color on the IS&T website (www.imaging.org) for a period of no less than two years from the date of publication.*

Valid Pixel Selection Using Distribution of CCD Camera Response

A real image includes error factors due to the non-uniformity of the CCD sensor, electrical signal instability, and camera noise.[12] Figure 2(a) shows a uniform green patch and is transformed to chromaticity coordinates under D65 illumination. In an ideal case, a patch of uniform chromaticity is represented by a single chromaticity coordinate. However, Fig. 2(b) shows that a uniform patch creates a cluster of chromaticity coordinates. Thus, to consider the total color tone, the camera response to the Gretag Macbeth Color Checker was investigated based on $r-g$ chromaticity coordinates under D65 illumination using a Sony DSC-D700 CCD camera in a dark booth. Figure 3(a) shows the 240 uniform color patches of the Gretag Macbeth Color Checker. Although ideally each color patch should be uniform, the *RGB* values of the captured image varied due to the non-uniformity of the camera response, as shown in Fig. 3(b), where the non-uniformity of the *RGB* response induced a cluster of $r-g$ chromaticity coordinates, rather than a single point, which is the major reason why the distribution of highlight region responses was similar to an ellipse. As such, a measure is needed that can consider the distribution of a cluster. Therefore, in the proposed highlight method, the covariance of the cluster is used to define the Mahalanobis distance, then the average value of the Mahalanobis distance among the 240 patches is used as the threshold ζ_{th} value which was 0.9129 in this case, to select valid camera responses,.

A block diagram of the proposed algorithm is shown in Fig. 4. First, an input image is segmented into high-

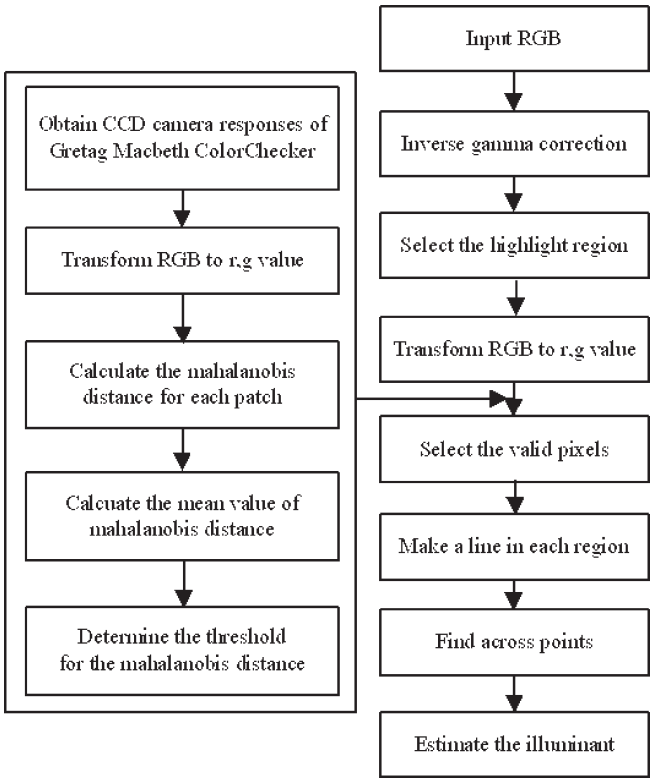

Figure 4. Block diagram of proposed algorithm.

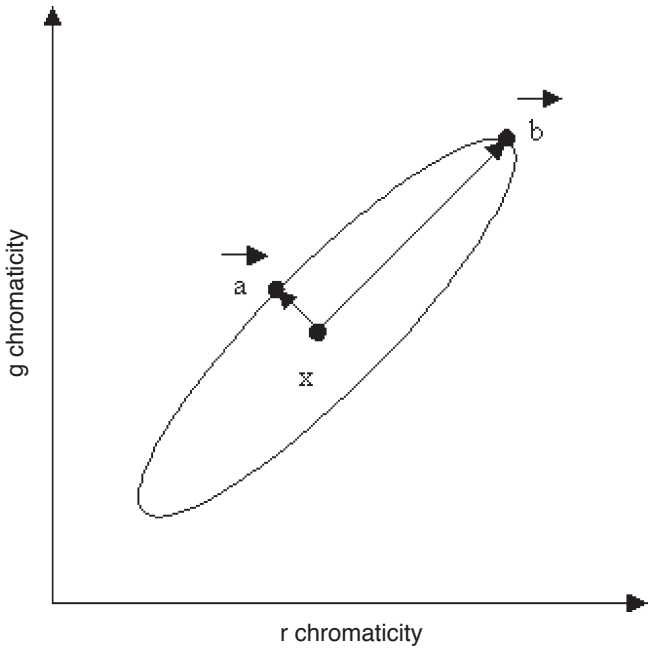

Figure 5. Relation of Mahalanobis and Euclidean distance in population.

light regions based on the *RGB* intensity, which in this article was determined as 20 × 20 pixels, to contain a single surface. Based on the $r - g$ chromaticity coordinates, an (r, g) value is calculated for each pixel in a highlight region using Eq. (5). Three representative values are then determined based on the intensity in each highlight region to effectively describe the feature of the cluster. New populations are selected in advance using the established threshold as a criterion for the three representative values. To obtain the threshold value, the standard deviation between the mean of the camera response and the cluster of the color tone for each Gretag Macbeth Color Checker patch is calculated, then the threshold is defined as the Mahalanobis distance for a pixel based on the standard deviation of the color tone. Next, the total tone is expanded by calculating the mean value for the Mahalanobis distance in each patch. As a result, valid pixels are selected from among the standard representatives in a highlight region.

Generally, the pixels of a highlight region form an elliptical shape based on their $r - g$ chromaticity coordinates. Thus, representatives need to be determined for selecting valid pixels from a highlight region. As such, Wandell's method[15] is used to determine cluster representatives. A cluster is divided by 0 ~ 30%, 0 ~ 70%, and 70 ~ 100% according to the intensity, based on the mean of the chromaticity values in each region. Therefore, valid pixels are selected within the Mahalanobis distance of the standard representatives.

Mahalanobis Distance Method

The Mahalanobis distance indicates the relation between clusters or the relation between a cluster and a pixel,[16]

$$M_d = \sqrt{\left(S - \bar{S}\right)^T \sum^{-1} \left(S - \bar{S}\right)} < \varsigma_{th}, \qquad (6)$$

where M_d is the Mahalanobis distance between an arbitrary pixel and the centroid, S is the location vector of an arbitrary pixel, $\bar{S}$ is the mean vector of the training set, and Σ is the variance-covariance matrix for the training set. Based on the distance calculated using Eq. (6), pixels are then selected that are close to the cluster's shape in a highlight region. This means that valid pixels are selected based on the Mahalanobis distance after analyzing the distribution of the CCD camera responses. Figure 5 shows an arbitrary population P and its representative x. When selecting two points a and b from the boundary of the population, $E(\vec{a} - \vec{x}) < E(\vec{b} - \vec{x})$, for the Euclidean distance. However, for the Mahalanobis distance, $M(\vec{a} - \vec{x}) = M(\vec{b} - \vec{x})$, where E and M are Euclidean distance and Mahalanobis distance, respectively. This is why the Mahalanobis distance is used to represent the characteristic of a population shape. After valid pixels are selected using the Mahalanobis distance, the line can be detected using a principal component analysis in each highlight region. The illumination can then be estimated using the intersection point of the lines.

Line Detection Using Principal Component Analysis

In general, a Hough transform[10,11,13] is used for line detection in highlight regions. However, if image noise is included, the result will inevitably involve an error. Therefore, the proposed algorithm uses a principal component analysis as the line detection method, since it is stronger than a Hough transform in the case of noise. Table I shows a performance comparison of a Hough transform and PCA for line detection based on experiments with three group images, as shown in Fig. 6. Figure 6(a) consists of foliage, Fig. 6(b) consists of faces, and Fig. 6(c) consists of fruits under unknown or known illumination. Each σ_r and σ_g is a standard deviation for the center point, and the line detection result is defined as

$$\eta = 1 - \sqrt{\sigma_r^2 + \sigma_g^2}$$

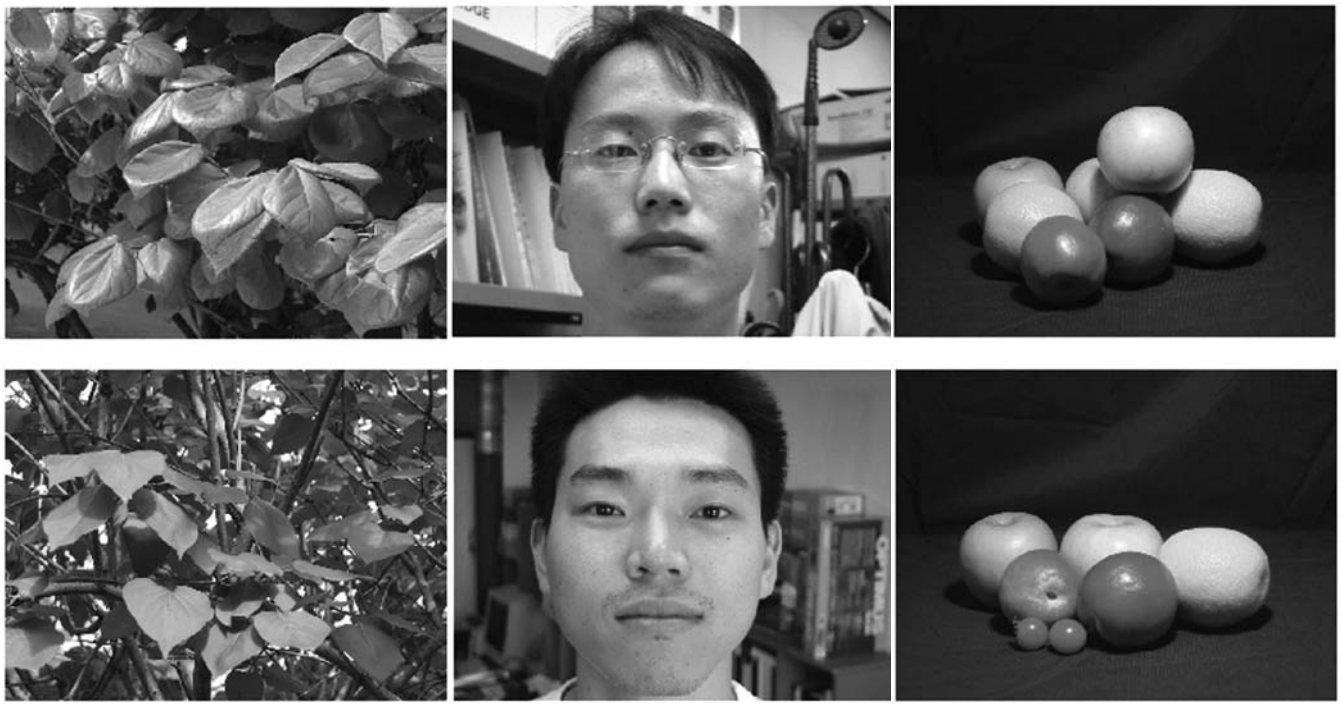

Figure 6. The test images used for experiment in Table I. *Supplemental Material—Figure 6 can be found in color on the IS&T website (www.imaging.org) for a period of no less than two years from the date of publication.*

TABLE I. Comparison between Hough Transform and PCA for Line Detection

	Group 1 (foliage)		Group 2 (face)		Group 3 (fruit)	
	Hough transform	PCA	Hough transform	PCA	Hough transform	PCA
σ_r	0.0082	0.0019	0.0822	0.0535	0.0847	0.0260
σ_g	0.0175	0.0172	0.0507	0.0282	0.1016	0.0154
η	0.9806	0.9826	0.9034	0.9395	0.8677	0.9697

with $\eta = 1$ as the best. The line for a cluster is detected using a statistical characteristic. As such, a principal component analysis is used to determine a single line based on the pixels of the $r - g$ chromaticity coordinates in a highlight region, i.e., for an arbitrary vector population,

$$X = \left[x_1 x_2 \cdots x_n\right]^T, \tag{7}$$

the mean vector of this population is then defined as,

$$m_x = E\{x\}, \tag{8}$$

and the covariance of the vector is

$$V_x = E\left\{(x - m_x)(x - m_x)^T\right\}, \tag{9}$$

where T is the transpose. The second order vector can then be analyzed using the pixels of the chromaticity coordinates. At this time, the eigenvalue of V_x is selected to determine the order of significance. i.e., a line is detected in a highlight region based on calculating the covariance value and significant eigenvalue for the highlight pixels. As a result of detecting the line using the principal component of the selected valid pixels, the camera noise is reduced, making the line accurate. Also, the estimated illumination error is smaller than the error of the CLS method, which is shown in detail through experiments.

Experiments

The proposed method was evaluated using a Sony DSC-D700 CCD camera, which was calibrated prior to the experiment. The image size was 640 × 480, the shutter speed was set to 1/45 s, and the f-number was 2.4. The experiment compared the lines obtained under four illuminations (Day, A, TL84, and CWF) in a Gretag Macbeth Judge II Booth. To compare the results, the pixels selected in the highlight regions were compared with the lines based on the chromaticity coordinates. In addition, the estimation error and reproduced images were compared for a quantitative result. Consequently, the images reproduced by the proposed method were visually closer to those obtained under the standard illumination than were those reproduced by conventional methods. In addition, the proposed method was able to accurately estimate the illumination using only a single real world image.

Results of Valid Pixel Selection in Highlight Region

Figure 7 shows the pixels selected after applying the proposed algorithm, where the pixels were selected using the average Mahalanobis distance based on the distribution of the camera response. Figure 7(a) represents the segmented regions in the test image, then Fig. 7(b) shows the distribution of pixels for a nose region in chromaticity space, while Fig. 7(c) shows the distribution of pixels for a cheek region in chromaticity space. The circles (•) denote the pixels selected by the proposed algorithm, whereas the squares (□) denote the pixels selected by the CLS method. Although the pixels in the highlight region were distributed based on chromaticity coordinates, the pixels selected

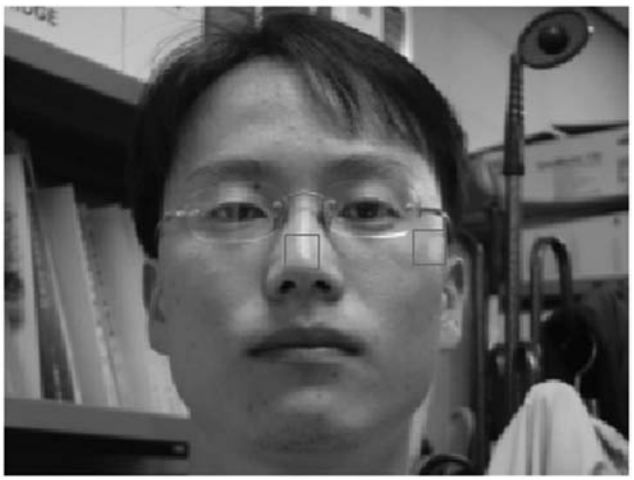

(a)

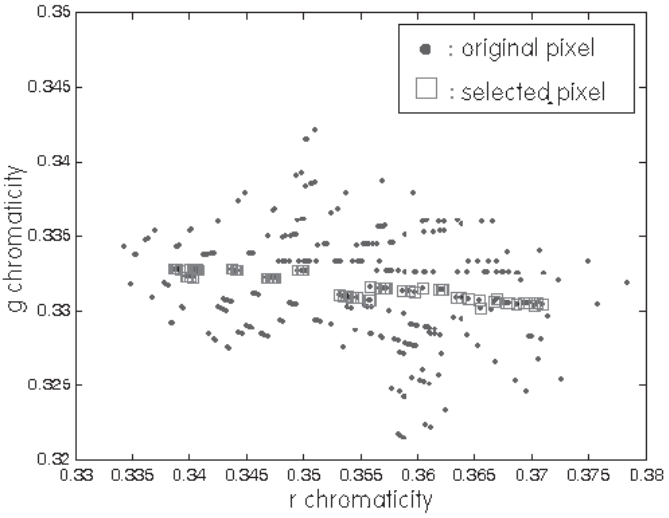

(b)

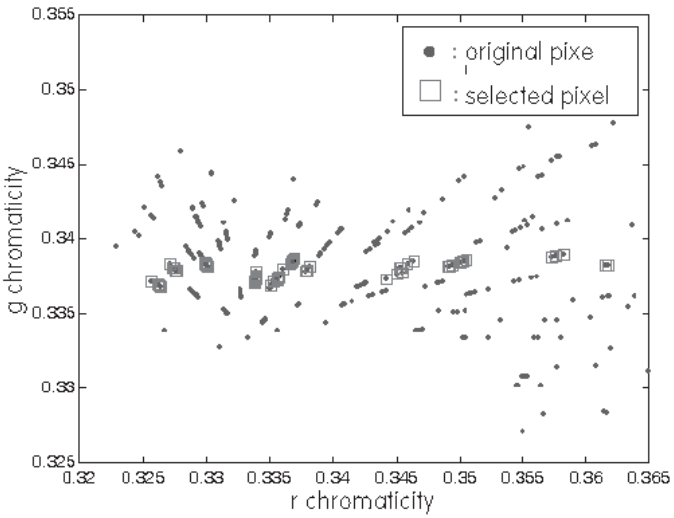

(c)

Figure 7. Pixel distribution in highlight regions; (a) test image, (b) pixels in nose region in chromaticity space, and (c) pixels in cheek region in chromaticity space. *Supplemental Material—Figure 7 can be found in color on the IS&T website (www.imaging.org) for a period of no less than two years from the date of publication.*

TABLE II. Comparison of Variation in Line Intersection Points in Highlight Region

	Illuminations	IPS method	CLS method	Proposed method
Day	$\hat{E}_r$	0.2772	0.3150	0.3112
	σ_r	0.2244	0.0200	0.0277
	$\hat{E}_g$	0.2774	0.3166	0.3164
	σ_g	0.1623	0.0370	0.0111
CWF	$\hat{E}_r$	0.3198	0.3464	0.3425
	σ_r	0.0719	0.0085	0.0109
	$\hat{E}_g$	0.3126	0.3466	0.3377
	σ_g	0.0679	0.0144	0.0087
TL84	$\hat{E}_r$	0.3634	0.3660	0.3693
	σ_r	0.2505	0.0381	0.0175
	$\hat{E}_g$	0.3607	0.3585	0.3658
	σ_g	0.0823	0.0268	0.0064
A	$\hat{E}_r$	0.3288	0.3529	0.3623
	σ_r	0.2523	0.0289	0.0203
	$\hat{E}_g$	0.3842	0.3368	0.3422
	σ_g	0.1205	0.0201	0.0034

by the proposed method represented a cluster. Table II shows a comparison of the variation in the line intersection points for the three methods. Each $\hat{E}_l$ and $\hat{E}_g$ is the estimated illumination in $r - g$ chromaticity space, while each σ_r and σ_g is the standard deviation for the estimated illumination. Even though the standard deviation is smaller, it is not necessarily accurate, despite being precise. However, the precision of the data contributes to the performance of the algorithm. As such, the proposed algorithms produced has relatively smaller standard deviation for the intersection points than the conventional algorithms.

Comparison of Illumination Estimation Error

Four images were obtained under different illuminations (Day, CWF, TL84, and A) in a light booth, and then the estimation error was calculated using the proposed and conventional methods. A visual comparison was made with reproducing the image under a standard illumination. The error in each illumination was shown after obtaining the same images under different illuminations, see Table III.

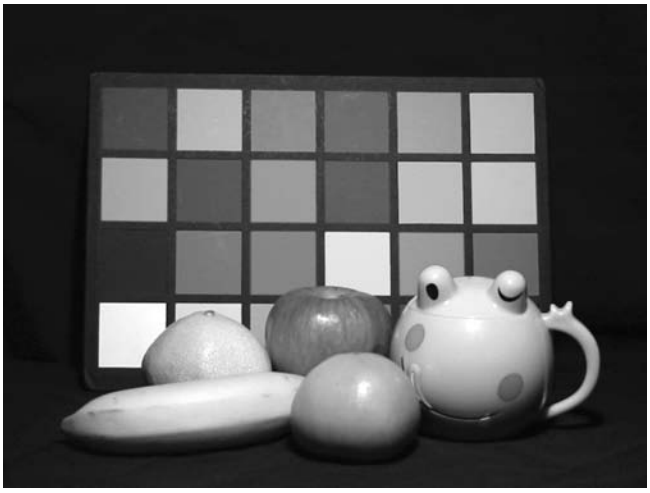

(a)

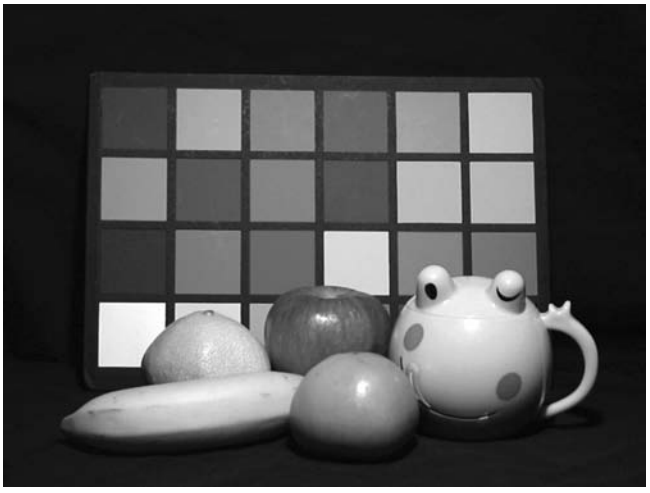

(b)

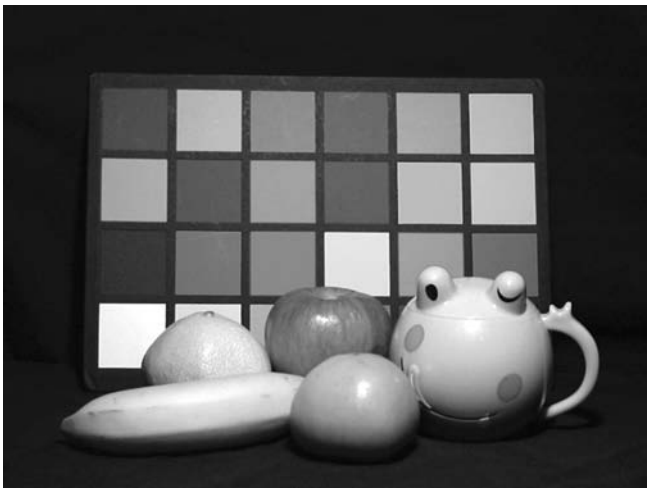

(c)

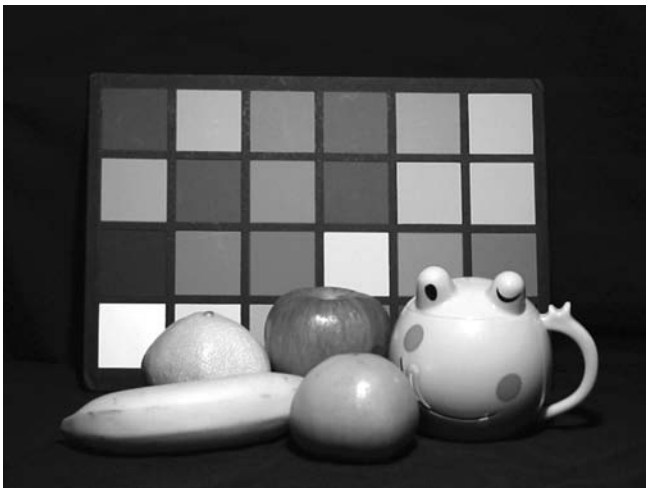

(d)

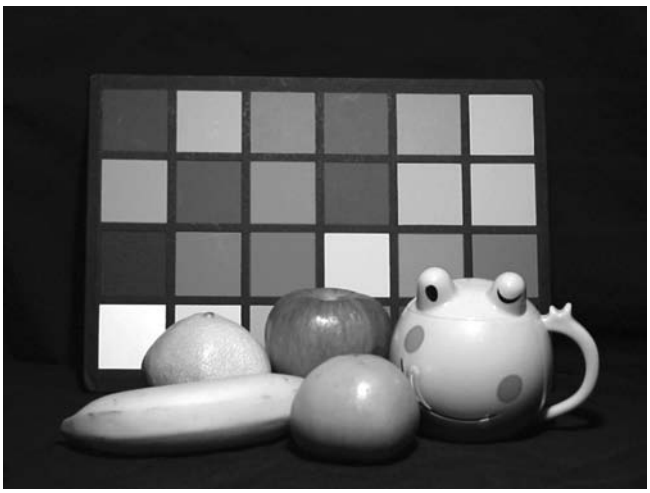

(e)

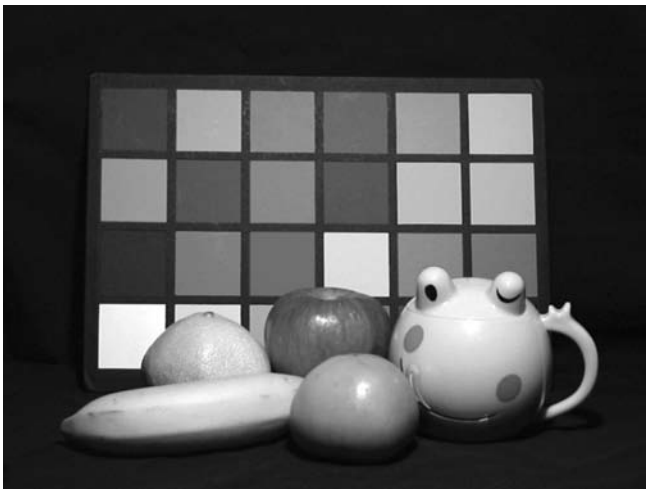

(f)

Figure 8. Results of image reproduction; (a) test image under A illumination, (b) image reproduced using measured illumination, (c) image reproduced using IPS method, (d) image reproduced using CLS method, (e) image reproduced using Inverse-Intensity method, and (f) image reproduced using proposed method. *Supplemental Material—Figure 8 can be found in color on the IS&T website (www.imaging.org) for a period of no less than two years from the date of publication.*

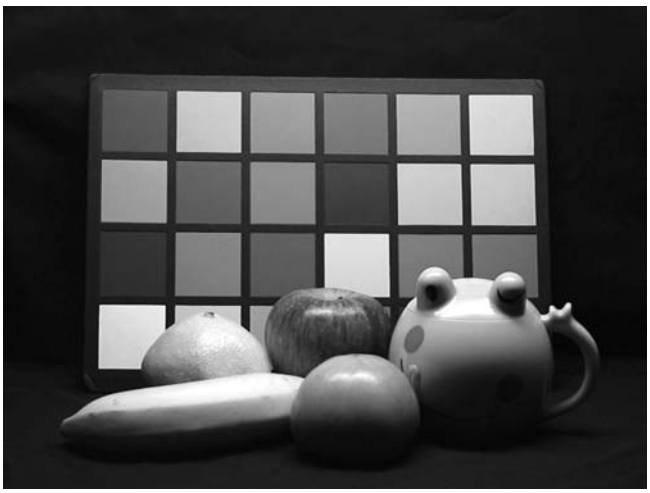

(a)

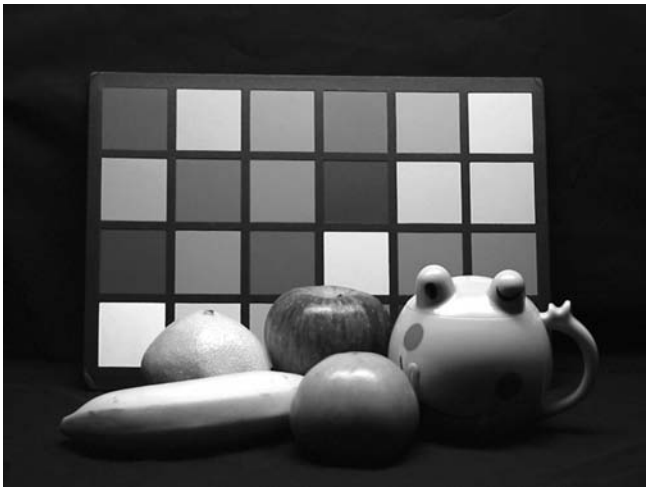

(b)

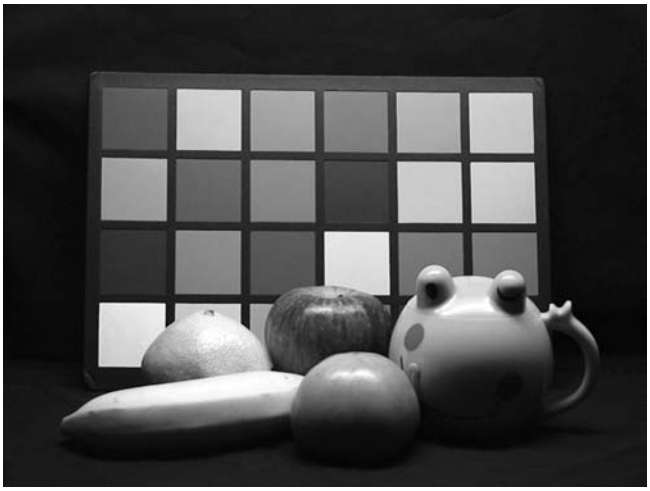

(c)

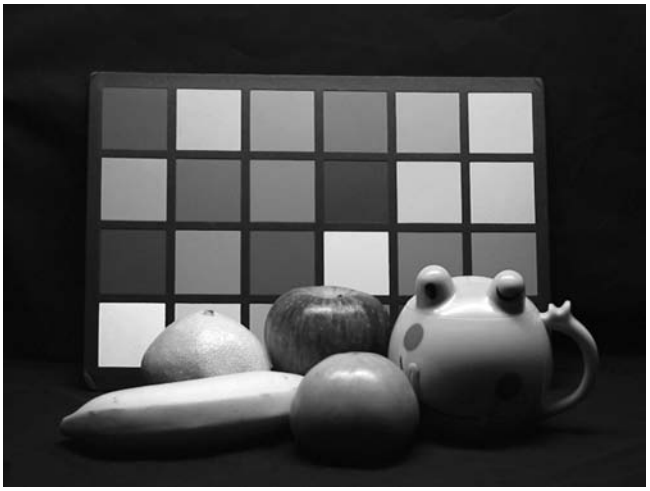

(d)

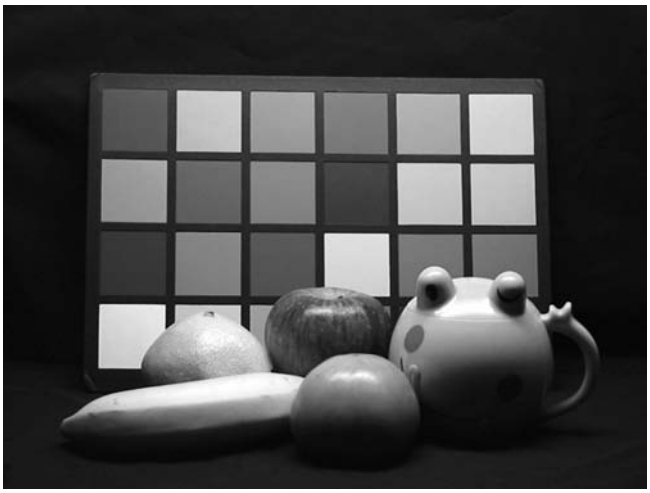

(e)

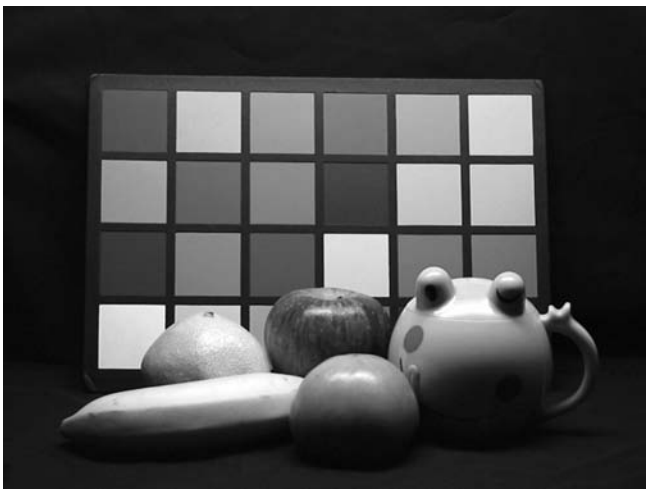

(f)

Figure 9. Results of image reproduction; (a) test image under CWF illumination, (b) image reproduced using the measured illumination, (c) image reproduced using IPS method, (d) image reproduced using CLS method, (e) image reproduced using Inverse-Intensity method, and (f) image reproduced using proposed method. *Supplemental Material—Figure 9 can be found in color on the IS&T website (www.imaging.org) for a period of no less than two years from the date of publication.*

TABLE III. Comparison of Color Difference According to Illuminations

Illumination	Retinex theory	IPS method	CLS method	Inverse-Intensity method	Proposed method
DAY	0.0438	0.0659	0.0241	0.0235	0.0227
CWF	0.0393	0.0422	0.0215	0.0140	0.0092
TL84	0.0528	0.0464	0.0432	0.0458	0.0427
A	0.0436	0.0841	0.0424	0.0412	0.0342

Table II shows the estimated illumination and standard deviation of the estimated illumination of the lines made by the chromaticity coordinates for the three methods in the same image under each illumination. Ideally, although the lines should cross at one point, this does not usually occur due to camera noise and the effect of the illumination. The results were similar to the chromaticity coordinates, so Table III shows the quantitative results for an accurate comparison. At this time, a reduced estimation error was confirmed for all the illuminations with the proposed method. The method of calculating the estimation error was as follows:

$$\Delta E_{eg} = \sqrt{\Delta r^2 + \Delta g^2}. \tag{10}$$

Each estimated error was 0.0227 (Day), 0.0092 (CWF), 0.0437 (TL84), and 0.0342 (A) for the four illuminations, which was smaller than that for all the conventional methods, except for the Inverse-Intensity method with A illumination. Then, reproductions were made under the standard illumination based on the results of the illumination estimation by the conventional methods and proposed method. In Figs. 8 and 9, each (a) image is captured under A and CWF illumination; each (b) image is reproduced based on the measured illumination; each (c) image is reproduced by the IPS method; each (d) image is reproduced by the CLS method; each (e) image is reproduced by the Inverse-Intensity method; and each (f) image is reproduced by the proposed method. The proposed method performed better than the conventional methods; although the proposed method was not always absolutely accurate in determining the measured illumination, the reproduced image was still visually similar to the measured image.

Conclusion

This article proposed a method for illumination estimation based on the distribution of CCD camera responses in a real world image. The proposed method analyzes the statistical data for the CCD camera responses, calculates the Mahalanobis distance for the camera responses, and then selects pixels based on the relation between the Mahalanobis distance and the cluster feature in a highlight region. In experiments, the images reproduced using the proposed method were visually more similar to under the standard illumination than those reproduced by the conventional methods. In addition, the illumination was estimated using only a single real world image. However, the proposed algorithm requires accurate segmentation of highlight regions and advance knowledge of the camera's characteristics through experimental settings, thereby limiting the applicability of the proposed method. Also, the proposed algorithm does not work well if there are two or more surfaces in a single highlight region or there is no highlight region or specular material in the image.

Acknowledgment. This work was supported by grant no. M10412000102-04J0000-03910 from the National Research Laboratory Program of the Korea Ministry of Science and Technology.

References

1. L. T. Maloney and B. A. Wandell, Color constancy: A method for recovering surface spectral reflectance, *J. Opt. Soc. Amer. A* **3**(1), 29-33 (1986).
2. M. D'Zmura, Color constancy: Surface color from changing illumination, *J. Opt. Soc. Amer. A* **9**(3), 490-493 (1992).
3. S. Tominaga and B. A. Wandell, Standard surface reflection model and illuminant estimation, *J. Opt. Soc. Amer. A* **6**(4), 576-584 (1989).
4. D. A. Forsyth, A novel algorithm for color constancy, *Int'l. J. Comp. Vision* **5**(1), 5-36 (1990).
5. S. Tominaga, S. Ebisui, and B. A. Wandell, Scene illuminant classification - Brighter is better, *J. Opt. Soc. Amer. A* **18**(1), 55-64 (2001).
6. S. Tominaga, Natural image database and its use for scene illuminant estimation, *J. Electron. Imaging* **11**(5) 434-444 (2002).
7. Y.-T. Kim, Y.-H. Cho, C.-H. Lee, and Y.-H. Ha, Estimation of spectral distribution of scene illumination from a single image with chromatic illuminant, *Proc. SPIE* **5008,** 171-181 (2003).
8. E. H. Land, The retinex theory of color perception, *Sci. Amer.* **237,** 108-129 (1977).
9. S. A. Shafer, Using color to separate reflection components, *Color Res. Appl.* **10**(4), 210-219 (1985).
10. H. C. Lee, Method for computing the scene-illuminant chromaticity from specular highlights, *J. Opt. Soc. Amer. A* **3**(10), 1694-1699 (1986).
11. R. T. Tan, K. Nishino, and K. Ikeuchi, Color constancy through inverse-intensity chromaticity space, *J. Opt. Soc. Amer. A* **21**(3), 321-334 (2004).
12. R. L. Baer, CCD requirement for digital photography, *Proc. IS&T's 2000 PICS Conference*, IS&T, Springfield, VA, 2000, pp. 26-30.
13. T. M. Lehmann and C. Palm, Color line search for illuminant estimation in real world scenes, *J. Opt. Soc. Amer. A* **18**(11), 2679-2691 (2001).
14. G. D. Finlayson and G. Schaefer, Solving for colour constancy using a constrained dichromatic reflection model, *Int'l. J. Comp. Vision* **42**(3), 127-144 (2001).
15. H. Z. Hel-Or and B. A. Wandell, Object-based illumination classification, *Pattern Recognition* **35**(8), 1723-1732 (2002).
16. P. J. Deer, P. W. Eklund, and B. D. Norman, A Mahalanobis distance fuzzy classifier, *Australian New Zealand Conference on Intelligent Information Systems*, ANZII96, Adelaide, Australia, 1996, pp. 18-20.